Cell Stem Cell
Article

BCL-2 Inhibition Targets Oxidative Phosphorylation and Selectively Eradicates Quiescent Human Leukemia Stem Cells

Eleni D. Lagadinou,[1] Alexander Sach,[1] Kevin Callahan,[1] Randall M. Rossi,[1] Sarah J. Neering,[1] Mohammad Minhajuddin,[1] John M. Ashton,[1] Shanshan Pei,[1,3] Valerie Grose,[1] Kristen M. O'Dwyer,[1,2] Jane L. Liesveld,[1,2] Paul S. Brookes,[4] Michael W. Becker,[1,2] and Craig T. Jordan[1,2,3,*]
[1]James P. Wilmot Cancer Center
[2]Division of Hematology/Oncology
[3]Department of Biomedical Genetics
[4]Anesthesiology Department
University of Rochester Medical Center, 601 Elmwood Avenue, Rochester, NY 14642, USA
*Correspondence: craig_jordan@urmc.rochester.edu
http://dx.doi.org/10.1016/j.stem.2012.12.013

SUMMARY

Most forms of chemotherapy employ mechanisms involving induction of oxidative stress, a strategy that can be effective due to the elevated oxidative state commonly observed in cancer cells. However, recent studies have shown that relative redox levels in primary tumors can be heterogeneous, suggesting that regimens dependent on differential oxidative state may not be uniformly effective. To investigate this issue in hematological malignancies, we evaluated mechanisms controlling oxidative state in primary specimens derived from acute myelogenous leukemia (AML) patients. Our studies demonstrate three striking findings. First, the majority of functionally defined leukemia stem cells (LSCs) are characterized by relatively low levels of reactive oxygen species (termed "ROS-low"). Second, ROS-low LSCs aberrantly overexpress BCL-2. Third, BCL-2 inhibition reduced oxidative phosphorylation and selectively eradicated quiescent LSCs. Based on these findings, we propose a model wherein the unique physiology of ROS-low LSCs provides an opportunity for selective targeting via disruption of BCL-2-dependent oxidative phosphorylation.

INTRODUCTION

Biological analyses of leukemia stem cells (LSCs) has been the focus of numerous studies over the past decade, with reports describing molecular, cellular, biochemical, and genetic properties in both human and mouse systems. It has been assumed to at least some extent that the biology of LSCs mirrors that of normal tissues, where malignant stem cells reside at the apex of a hierarchical developmental structure. Indeed, key stem cell properties such as self-renewal are readily evident in stem cells from multiple tumor types (Magee et al., 2012). In addition, quiescent cell cycle status, a very well described feature of normal hematopoietic stem cells (HSCs), also appears to be a central property of functionally defined acute myeloid leukemia (AML) stem cells (Saito et al., 2010). Further, several molecular mechanisms that regulate normal stem cell properties are also frequently active (and/or aberrant) in cancer cell types as well (Magee et al., 2012). These observations have led investigators to attempt targeting of LSC populations based on properties that are thought to be shared among normal and tumor primitive cells and are conserved from patient to patient.

Despite the similarities noted above, it has become increasingly clear that primitive cancer cell types possess important differences from normal tissues, some of which run counter to conventional views of stem cell biology. For example, recent studies have shown that cell surface immunophenotype can vary widely among specimens derived from primary AML patients, and that commonly used stem cell antigens such as CD34 and CD38 do not show consistent levels of expression on LSCs (Eppert et al., 2011; Sarry et al., 2011). Thus, unlike normal hematopoietic tissues, which show substantial interspecimen similarities, some of the biological properties of independent LSCs may be highly disparate and/or unstable.

Given the observations outlined above, we sought to better define fundamental aspects of LSC biology, which are conserved irrespective of interpatient or intrapatient heterogeneity. To this end, we investigated energy metabolism, a basic requirement of any cell type. Cancer cells appear to commonly acquire aberrancies in energy metabolism and cellular redox state (Cairns et al., 2011). In contrast to their normal counterparts, cancer cells tend in the presence of oxygen to employ glycolysis instead of aerobic mitochondrial respiration to generate energy (Warburg, 1956). Notably, in at least some instances, cancer cells generate increased levels of reactive oxygen species (ROS) (Trachootham et al., 2008). This notion has provided the impetus to explore redox modulation as a therapeutic target in cancer, with the rationale that pro-oxidants may eradicate tumor cells by pushing them beyond the limits of viability (Trachootham et al., 2009). However, while such tumor-related metabolic adaptations characterize bulk tumor tissues, it is unclear whether cancer stem cells (CSCs) also exhibit an increased oxidative state. Indeed, previous studies by Diehn et al. (2009) demonstrated that breast cancer cells enriched

for the breast CSC-related $CD24^{-}/CD44^{+}$ phenotypic profile showed lower levels of ROS than the "non $CD24^{-}/CD44+$" cells. Gaining further insights into the metabolic properties of CSCs may reveal physiological dependencies that can be targeted for therapy.

In the present study we used primary human AML specimens and a stringent xenograft assay to investigate the oxidative state and the bioenergetic properties of LSCs. We show that in contrast to the nontumorigenic cells, the majority of self-renewing and chemotherapy-resistant primitive leukemic populations are quiescent tumor subsets characterized by a low rate of energy metabolism and a low cellular oxidative status (termed "ROS-low"). Surprisingly, ROS-low cells are unable to utilize glycolysis when mitochondrial respiration is inhibited. Thus, we show that the maintenance of mitochondrial function is essential for LSC survival. Finally, we demonstrate a unique role for BCL-2 in ROS-low cell mitochondrial respiration, and show that small molecule BCL-2 inhibitors can effectively target chemotherapy-resistant LSCs by impairing their energy generation capacity and redox control. Our findings indicate it is feasible to eradicate therapy-resistant LSC populations by targeting their unique metabolic dependencies.

RESULTS

Stem Cell Properties of Primary AML Populations Isolated on the Basis of Intracellular ROS

To characterize leukemia cells with differing oxidative state, we employed a method previously reported by Jang and Sharkis (2007). In this study, the authors used cell sorting based on the relative fluorescence of redox-sensitive probes to isolate HSCs with differing endogenous ROS levels. Since a number of recent studies have highlighted that LSCs may display disparate phenotypic patterns besides $CD34^{+}/CD38^{-}/CD123^{+}$ (Eppert et al., 2011; Sarry et al., 2011), in performing our initial analyses of ROS levels in primary AML samples, we did not rely on standard phenotypic profiles, but rather examined the entire leukemic population. By employing several redox-sensitive probes commonly used to measure intracellular ROS (CM-H2DCFDA, CellROX, MitoSox, Mitotracker, and DHE) we consistently observed substantial heterogeneity in the redox staining profile of AML specimens (Figure 1A and Figures S1A and S1B available online). Since the fluorescent dyes CM-H2DCFDA and CellROX provide a broader measure of intracellular redox levels, we used those two dyes to sort AML specimens into subsets with low and high endogenous ROS (defined as the 15% dimmest and brightest dye fluorescence distribution as shown in Figure 1A) and then analyzed the two populations for stem cell properties.

A critical feature of both normal and leukemia primitive populations is quiescence, as increased proliferation can lead to exhaustion of stem cell function (Ito et al., 2006; Tothova et al., 2007). We hypothesized that quiescence may reduce LSC metabolic activity and thus lower ROS production, so slowly proliferating LSCs should be enriched in the redox low compartment. To investigate this issue, we colabeled sorted ROS-low and ROS-high fractions with anti-Ki67 and 7AAD to evaluate cell cycle status. As shown in Figures 1B and 1C, leukemic ROS-low cells are preferentially enriched for G_0 quiescent cells. This finding was corroborated by analyses of cell cycle components, which demonstrated reduced expression of CDK1; cyclins A2, B2, D3 and E2; and increased expression of the cell cycle inhibitor p27 in ROS-low cells (Figures S1C and S1D). ROS-low cells also showed reduced expression of the MAPK kinase phospho-p38, which is associated with redox state regulation and cell cycle activity in normal hematopoiesis (Figure S1D) (Ito et al., 2006). Interestingly, ROS-low subsets isolated from the M9-ENL1 AML cell line and from normal marrow $CD34^{+}$ cells were also more quiescent as compared to corresponding ROS-high cells (Figure S1E), indicating that the association between lower ROS and quiescence is conserved in both cell lines and normal HSCs.

To assess whether AML cells with lower endogenous ROS are enriched for primitive leukemia cells, we first performed in vitro colony assays to determine colony-forming units (CFUs). In four evaluable AML samples, the leukemic cells with lower ROS gave growth to more CFUs in comparison to ROS-high or total AML cells (Figure 1D), suggesting enrichment of primitive cells in the ROS-low compartment. To functionally evaluate LSC potential, xenograft studies were performed using transplantation of primary human cells into immune deficient *NOD/SCID-IL2R*$\gamma^{-/-}$ (NSG) mice. As shown in Figure 1E, LSC activity (i.e., successful engraftment of NSG mice) is readily evident in all ROS-low AML subsets evaluated (five of five independent specimens). Notably, in two of five specimens we also detected some LSC activity (albeit at lower levels) with ROS-high AML cells, suggesting that functionally defined primitive leukemia populations can exist across a relatively broad ROS gradient in at least some cases. However, the leukemic subsets isolated from the lowest end of the ROS range were consistently more enriched for LSC activity as compared to AML cells containing high levels of ROS (Figure 1E and Figure S1F). Indeed, in transplantation experiments (Figure 1E), despite the fact that AML ROS-low cells were injected in NSG mice at a 5-fold lower dose than unfractionated total AML cells (Table S2), the ROS-low population engrafted at levels comparable to the total AML cells (AML ROS-low = 44.6 ± 38 versus total AML = 51 ± 38, $p = 0.122 > 0.05$, $n = 5$). Further, to address whether ROS-low cells fulfill the stem cell criterion of long-term self-renewal, we performed serial transplantation studies in secondary mouse recipients. ROS-low leukemic cells reestablished AML in the secondary recipients in all cases, thus confirming their leukemic stem cell potential (Table S3). Interestingly, in two out of three AML specimens where ROS-high AML cells engrafted at levels that allowed comparative serial transplantation analyses, we observed long-term self-renewal potential in secondary recipients, suggesting that LSCs are significantly fewer but evident within the redox high leukemic compartment (Table S3). Since normal HSCs have been suggested to reside in a reduced oxidized state, we next tested if the increased engraftment potential of the ROS-low AML subset resulted from contributing HSCs (Tothova et al., 2007). To this end we analyzed the human cells from mice engrafted with ROS-low or ROS-high AML cells (patient sample #1) for expression of mutant nucleophosmin (NPM), which is a frequently observed leukemia marker (Falini et al., 2007). Engrafted AML cells from both leukemic subsets were positive for this marker (Figure S1G), thus confirming the leukemic origin of engrafted cells in both cases.

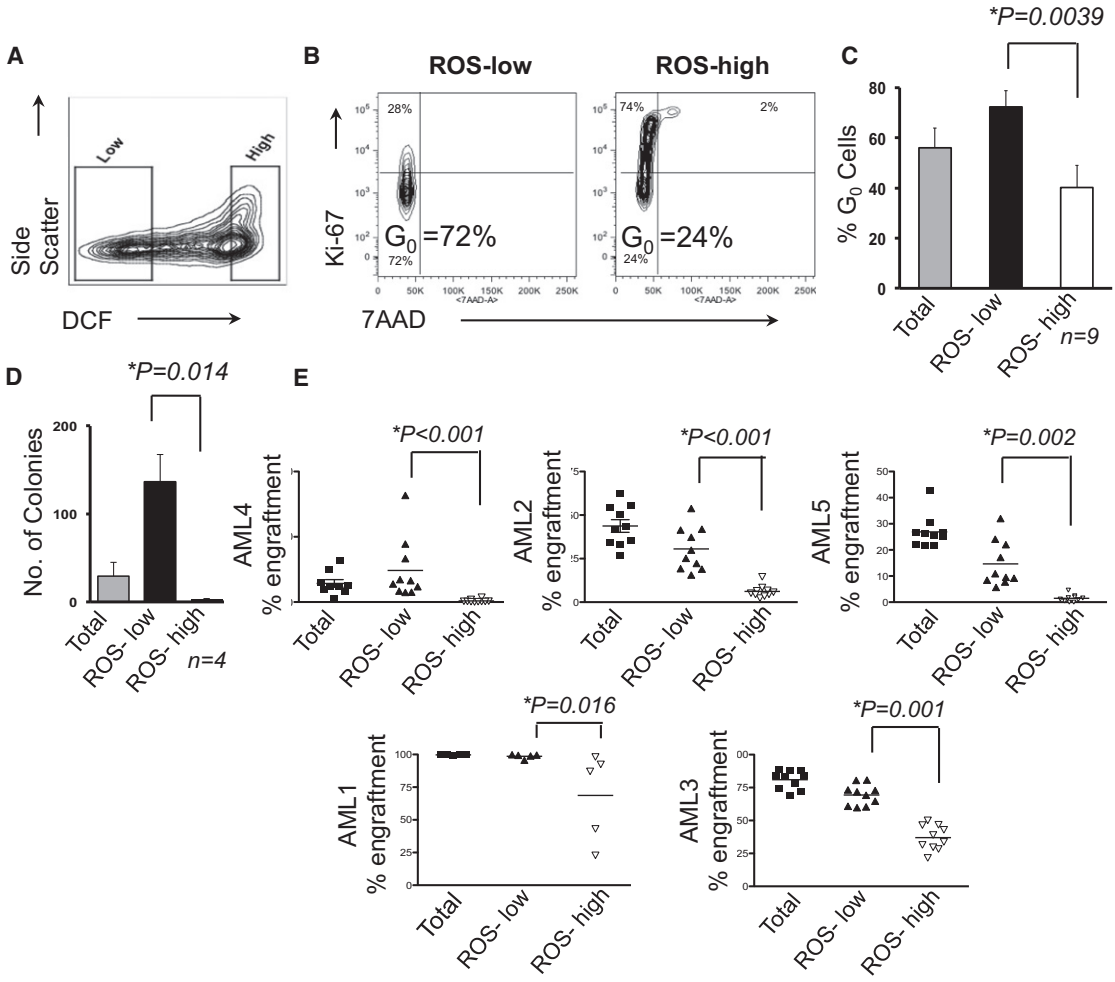

Figure 1. Stem Cell Properties of Leukemia Cells Isolated on the Basis of Intracellular ROS

(A) CM-H2DCFDA labeling of primary AML specimen. DCF; CM-H2DCFDA. See also Figures S1A and S1B.

(B) Representative cell cycle analysis of sorted ROS-low and ROS-high primary AML subsets performed by Ki67 and 7AAD labeling.

(C) Cell cycle analyses from n = 9 primary AML samples are summarized. Mean ± SEM percentages of G_0 cells are plotted. See also Figures S1C–S1E.

(D) Number of colonies per 5 × 10^4 cultured cells in total AML, ROS-low, and ROS-high subsets. Mean ± SEM values of n = 4 primary AML specimens are plotted.

(E) Total AML, ROS-low, and ROS-high leukemia subsets were transplanted into NSG mice at a constant cell ratio of 5:1:1 as described in the Experimental Procedures. Mice were killed 6–8 weeks later, and their marrow was analyzed by flow cytometry for engraftment of human leukemia cells. Results from n = 5 independent AML specimens are shown. See also Figure S1F.

We next asked if AML cells containing lower levels of ROS are enriched for the $CD34^+/CD38^-$ phenotypic profile, which is commonly associated with stem cells in both normal and leukemic hematopoiesis. We found an increased percentage of $CD34^+/CD38^-$ cells in the ROS-low subset as compared to those in the ROS-high, but no significant enrichment of this phenotypic profile when the ROS-low cells where compared to the total AML population (Figure S1H). Further, analysis of AML specimens with an additional collection of antibodies associated with primitive cell types (CD123, CD33, CD117, CD90, and CD44) did not reveal any clear association between surface expression profile and a lower oxidative state (data not shown).

Taken together, these findings indicate that endogenous ROS levels can be used as a tool to prospectively isolate LSC-enriched populations. To identify properties of LSCs that can be targeted for therapy, we therefore used endogenous ROS sorting to enrich for LSCs, and studied mechanisms controlling energy metabolism in LSC-enriched populations.

LSC-Enriched Primary Populations Are Metabolically Dormant and Are Dependent on Oxidative Respiration rather than Glycolysis for Energy Generation

To gain insights into the metabolic regulation of LSCs, we performed bioenergetic analyses in ROS-low and ROS-high primary AML specimens. We first investigated the relative dependence of the ROS-low AML cells to the two major energy-generating pathways: mitochondrial oxidative phosphorylation (OXPHOS) and glycolysis. To this end, we used the Seahorse XF24 extracellular flux analyzer to measure the oxygen consumption rate (OCR) indicative of OXPHOS, and the lactate production indicative of glycolysis (extracellular acidification rate; ECAR). As shown in Figure 2A, LSC-enriched

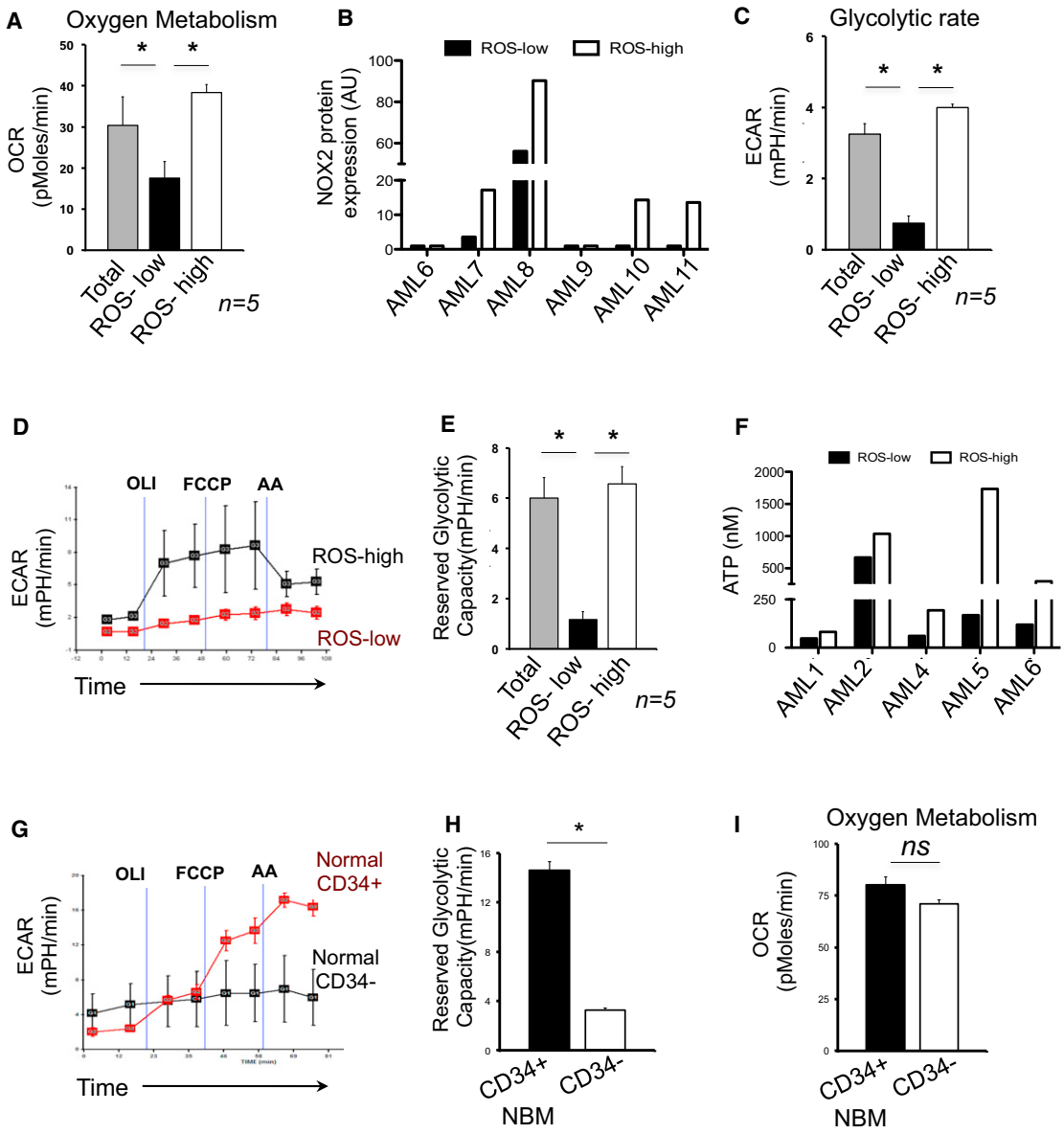

Figure 2. Bioenergetic Analyses in LSC-Enriched versus Bulk Leukemic and Normal Primitive Populations

(A) Basal oxygen consumption rate (OCR) in total AML and ROS-low cells versus ROS-high subsets, as evaluated by the Seahorse XF24 extracellular flux analyzer. Five replicate wells of 5 × 10^5 ROS-low and ROS-high leukemic cells were analyzed. Mean ± SEM values from n = 5 AML specimens are plotted. *p ≤ 0.05. See also Figure S2.

(B) Protein expression levels of the NADPH oxidase subunit NOX2 (gp91phox) in ROS-low versus ROS-high primary subsets, as evaluated by flow cytometry. Mean fluorescence intensity values are plotted. AU, arbitrary units.

(C) Mean ± SEM values of baseline extracellular acidification rate (ECAR) indicative of glycolytic rate in n = 5 primary AML specimens. *p ≤ 0.05.

(D) Reserved glycolytic capacity in ROS-low cells (red) versus ROS-high AML cells (black) in a primary AML specimen. ECAR was measured without (first two measurements) and in the presence of (measurements 3–8) the mitochondrial inhibitors oligomycin (OLI, 1 μg/ml), FCCP (1 μM), and Antimycin (AA, 5 μM). Basal ECAR is calculated as the mean of measurements 1 and 2. Reserved glycolytic capacity is determined as the mean of the measurements 5 and 6 minus the mean of the first two measurements.

(E) Mean ± SEM values of reserved glycolytic capacity in n = 5 primary AML specimens. *p ≤ 0.05.

(F) Mean values of baseline ATP levels in ROS-low versus ROS-high leukemia cells.

(G) Representative experiment of reserved glycolytic capacity in normal $CD34^+$ (red) versus $CD34^-$ (black) marrow cells.

(H) Plot of mean ± SEM values of reserved glycolytic capacity from two independent experiments in $CD34^+$ versus $CD34^-$ normal subsets. Reserved glycolytic capacity was determined as in (D). *p ≤ 0.05.

(I) Basal oxygen consumption rate (OCR) of normal marrow $CD34^+$ versus $CD34^-$ subsets. Mean ± SEM values are plotted.

ROS-low cells showed a significantly lower OCR rate, indicative of lower oxidative metabolism, as compared to the total and ROS-high AML cells. While oxidative processes occur mainly in mitochondria, oxidative activity can also be found in the cytoplasmic membrane due to the presence of the NADPH oxidases (Hole et al., 2010). Therefore, we evaluated the protein expression of NADPH oxidase subunit NOX2 (gp91phox) by flow cytometry. As shown in Figure 2B, NOX2 levels were found to be quite low in ROS-low cells, indicating mitochondria as the primary site of oxidative metabolism in LSC-enriched populations. AML ROS-low cells isolated based on the fluorescence of the redox dye CM-H2DCFDA also showed reduced labeling with the mitochondrial-specific redox probe MitoSox-Red, indicating a lower content of mitochondrial-derived ROS (Figure S2). We next examined relative rates of glycolysis and observed that ROS-low cells are substantially less active with respect to this anaerobic form of energy production as well (Figure 2C). While the basal rate of glycolysis in ROS-low cells is low, it is possible that under certain conditions (i.e., in hypoxic niches in vivo) LSCs might compensate for low OXPHOS by upregulating glycolysis. To investigate this issue we measured lactate generation indicative of the cellular glycolytic rate after treatment of cells with the mitochondrial respiration inhibitors oligomycin (OLI) and FCCP. OLI and FCCP inhibit mitochondrial respiration and force cells to the glycolytic pathway to maintain energy supply, so treatment with these agents is indicative of the reserved cellular glycolytic potential. Surprisingly, LSC-enriched ROS-low AML cells showed a significantly decreased potential to upregulate the glycolytic machinery and thus sustain energy generation when mitochondrial energy production was inhibited (Figures 2D and 2E). In agreement with our bioenergetic data, ROS-low cells showed significantly decreased ATP levels in all samples evaluated (Figure 2F).

To determine whether the metabolic status of ROS-low AML cells represents an aberrant condition, we performed comparative bioenergetic analyses of normal bone marrow $CD34^+$ progenitors isolated from healthy volunteers. A recent study showed that murine hematopoietic stem populations are predominantly glycolytic (Simsek et al., 2010), but to our knowledge the bioenergetic profile of human marrow progenitors has not been previously investigated. We found that, in contrast to AML ROS-low cells, normal $CD34^+$ cells are metabolically active cells with baseline glycolysis and OXPHOS rates similar to $CD34^-$ cells (Figures 2G and 2I). Further, normal $CD34^+$ progenitors preferentially (in comparison with $CD34^-$ cells) upregulate glycolysis when mitochondrial OXPHOS is blocked (Figures 2G and 2H).

Taken together, our metabolic analyses indicate that LSC-enriched subsets are metabolically dormant tumor populations that reside in a substantially decreased energetic state. Importantly, our findings further suggest that in contrast to normal progenitor cells, LSC-enriched subsets may paradoxically depend more on mitochondrial respiration rather than glycolysis to meet their energy demands and maintain their survival.

BCL-2 Is Upregulated in LSC-Enriched Primary AML Populations

To investigate mechanisms that control oxidative state and metabolic processes in ROS-low and ROS-high populations, we performed gene expression studies using RNA-seq-based methods. Since our findings indicated LSC-enriched populations contained lower levels of ROS, we investigated if upregulation of antioxidant genes represents a prominent feature of ROS-low AML cells. We found only a small number of genes related to antioxidant defenses to be significantly altered in ROS-low AML cells, none of which were consistently upregulated in the ROS-low population (Figure S3A). We next investigated the relative expression of genes related to mitochondria and energy metabolism. In agreement with an important role of mitochondrial metabolism in LSCs, we found several mitochondrial-related genes upregulated in ROS-low cells. These included the *SLC25A42* and *SLC25A38* mitochondrial carriers that transport metabolites and amino acids across the mitochondrial membrane, and the gene *FIS1*, which is critical for mitochondrial dynamics and fission (Figure 3A) (Westermann, 2010). Intriguingly, we found that the LSC-enriched ROS-low population expressed significantly higher levels of *BCL-2* (Figure 3A). We validated this initial observation using quantitative PCR in a larger AML sample cohort (Figure 3B). *BCL-2* mRNA expression correlated with protein expression, as ROS-low AML cells expressed higher levels of BCL-2 protein (Figure 3C), whereas they showed no significant upregulation of other antiapoptotic BCL-2 family members including BCL-X_L and MCL-1 (Figures S3B and S3C). Parallel analyses of BCL-2 gene expression in normal marrow specimens showed, in agreement with previous observations (Delia et al., 1992), that normal $CD34^+$ progenitors express significantly higher levels of BCL-2 as compared to more differentiated $CD34^-$ cells (Figures S3D–S3F). To investigate the extent to which normal $CD34^+$ progenitors share the BCL-2 expression profile observed in leukemic cells, we further examined BCL-2 levels in normal $CD34^+$ ROS-low versus ROS-high populations. To this end, we enriched for $CD34^+$ progenitors using an immunomagnetic affinity column and then isolated $CD34^+$ ROS-low and ROS-high populations by flow cytometry. $CD34^+$ ROS-low cells showed a modest increase in BCL-2 mRNA expression as compared to $CD34^+$ ROS-high, but we found no difference in the BCL-2 protein levels among the two populations in three independent experiments (Figures S3G–S3H). Based on these data, we conclude there is no differential activity of BCL-2 between normal ROS-low and ROS-high compartments.

The upregulation of BCL-2 in the LSC is potentially important, since (1) BCL-2 has an established role as an inhibitor of the mitochondrial-initiated proapoptotic pathway and thus can represent an important contributor in the chemoresistance properties of LSCs (Del Poeta et al., 2003), and (2) recent evidence points to a noncanonical activity of BCL-2 in regulating oxidative state and mitochondrial metabolism (Chen and Pervaiz, 2007). Thus, elevated BCL-2 could contribute to key functional properties of LSCs.

BCL-2 Inhibition Targets LSC Mitochondrial Energy Generation

To investigate the role of BCL-2 in the metabolic homeostasis of primitive leukemia cells, we determined the bioenergetic properties of primary AML cells treated with BCL-2 pharmacologic inhibitors. We found that within minutes of treatment, the BCL-2 inhibitor ABT-263 induces severe impairment of OXPHOS

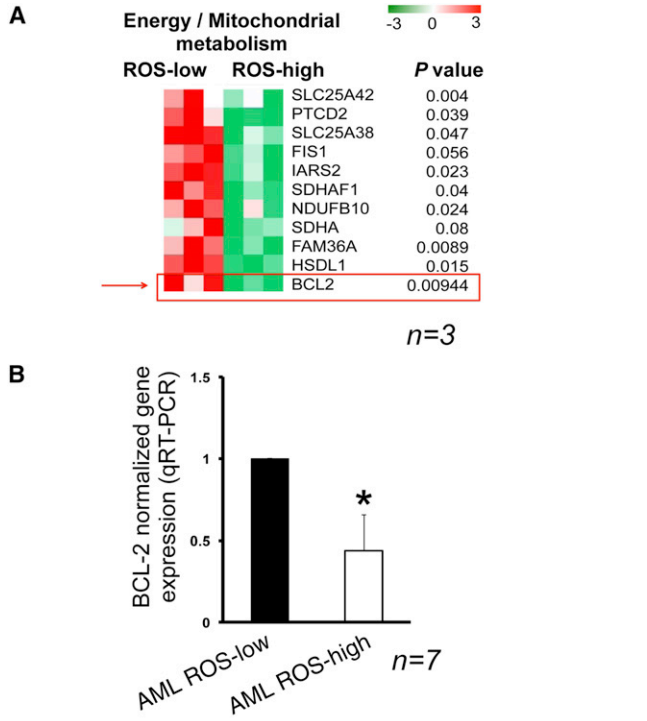

Figure 3. BCL-2 Is Upregulated in LSC-Enriched Primary AML Populations

(A) Heat map of relative expression of energy and mitochondrial-related genes in ROS-low AML cells compared to ROS-high cells (green = downregulated, red = upregulated). RNA was isolated from each purified population from n = 3 independent AML specimens and subjected to whole transcriptome analysis (RNA-seq) as described in the Experimental Procedures. The two-sample homoscedastic, independent t test was used for comparing the states described. $p \leq 0.05$ was set as significant. See also Figures S3A and S3B.

(B) Normalized *BCL-2* gene expression determined by quantitative real-time PCR in ROS-high as compared to ROS-low AML subsets. Mean ± SEM values of n = 7 primary AML specimens are presented (*$p \leq 0.05$).

(C) Western blot analyses of BCL-2 protein levels in ROS-low versus ROS-high leukemia cells. See also Figures S3C–S3H.

in primary unfractionated AML cells (Figure 4A and Figure S4A). Similarly, a second chemically distinct BCL-2 inhibitor, obatoclax, also inhibited oxidative respiration in leukemia cells (Figure S4B), albeit to a lesser extent than ABT-263. This effect is accompanied by a robust glycolytic response (Figure 4D), indicating that glycolysis is a compensatory mechanism activated upon inhibition of OXPHOS by BCL-2 inhibitors. ABT-263 similarly impaired OXPHOS in the LSC-enriched ROS-low cells (Figure 4B). However, in agreement with our previous findings showing that ROS-low AML cells have reduced reserved glycolytic capacity (Figures 2D and 2E), ROS-low cells were not able to induce glycolysis (Figure 4D). These findings suggested that ABT-263 should selectively inhibit energy generation in the ROS-low population. Indeed, ABT-263 rapidly depleted cellular ATP in the ROS-low AML subset (Figure 4E, left panel), whereas it had no effect in the ATP content of the ROS-high population (Figure 4E, middle panel).

To investigate the role of BCL-2 in normal populations, we tested the effect of ABT-263 treatment in $CD34^+$ cells from healthy donors. As shown in Figure 4C, OCR was impaired, albeit to a lesser extent than that observed in leukemic cells. In agreement with our data showing that normal $CD34^+$ cells possess reserve glycolytic capacity (Figure 2H), we detected a clear upregulation of glycolysis in normal $CD34^+$ subsets in response to ABT-263-induced OXPHOS inhibition (Figure 4D). Importantly, evaluation of the effect of ABT-263 on the ATP content of normal $CD34^+$ progenitors revealed no significant impact, unless ABT-263 was combined with the glycolysis inhibitor 2-deoxyglucose (2-DG) (Figure 4E, right panel). The combination of ABT-263 and 2-DG induced a decrease in the ATP content of normal $CD34^+$ cells to levels similar to those observed in ROS-low AML cells treated with ABT-263 alone. These data indicate that glycolytic capacity represents an important biological property that distinguishes ROS-low AML cells from normal $CD34^+$ cells.

To more directly address the role of BCL-2 in the oxidative respiration of leukemia cells, we employed an shRNA strategy to genetically reduce gene expression. Using lentiviral-mediated gene transfer, we expressed *BCL-2* shRNAs in primary AML cells and the U937 leukemia cell line (Figure S4C). Primary leukemic and U937 cells transduced with *BCL-2* shRNA showed a significantly reduced basal oxygen consumption rate as compared to cells transduced with a control vector (Figure 4F and Figure S4D), indicating that BCL-2 is a positive regulator of OXPHOS in leukemia cells. Further, the capacity of ABT-263 to suppress oxidative respiration was markedly decreased in *BCL-2* shRNA-transduced primary AML cells as compared to vector control cells (Figure 4G and Figure S4E). Knocking down *BCL-X_L* (the other known target of ABT-263) (van Delft et al., 2006) by specific shRNA did not have a significant effect on the OXPHOS of primary leukemic cells (Figure S4F). Taken together, these findings strongly indicate that inhibition of oxidative respiration induced by treatment with ABT-263 is mediated by inhibition of BCL-2.

BCL-2 Inhibition Induces Cell Death in the LSC Compartment

Based on our finding that BCL-2 inhibition induced mitochondrial dysfunction and energy depletion in ROS-low cells, we next asked if oxidation was promoted. To this end, we measured mitochondrial ROS levels using the mitochondrial superoxide detector MitoSox-Red. We found that ABT-263 induces a clear upregulation of mitochondrial ROS selectively in LSC-enriched ROS-low cells (Figure 5A and Figure S5). As BCL-2 inhibition increased the oxidative state of ROS-low cells, we investigated whether changes in antioxidant defenses were evident. We found that ABT-263 treatment resulted in decreased levels of reduced glutathione (GSH) in the ROS-low subset (Figure 5C).

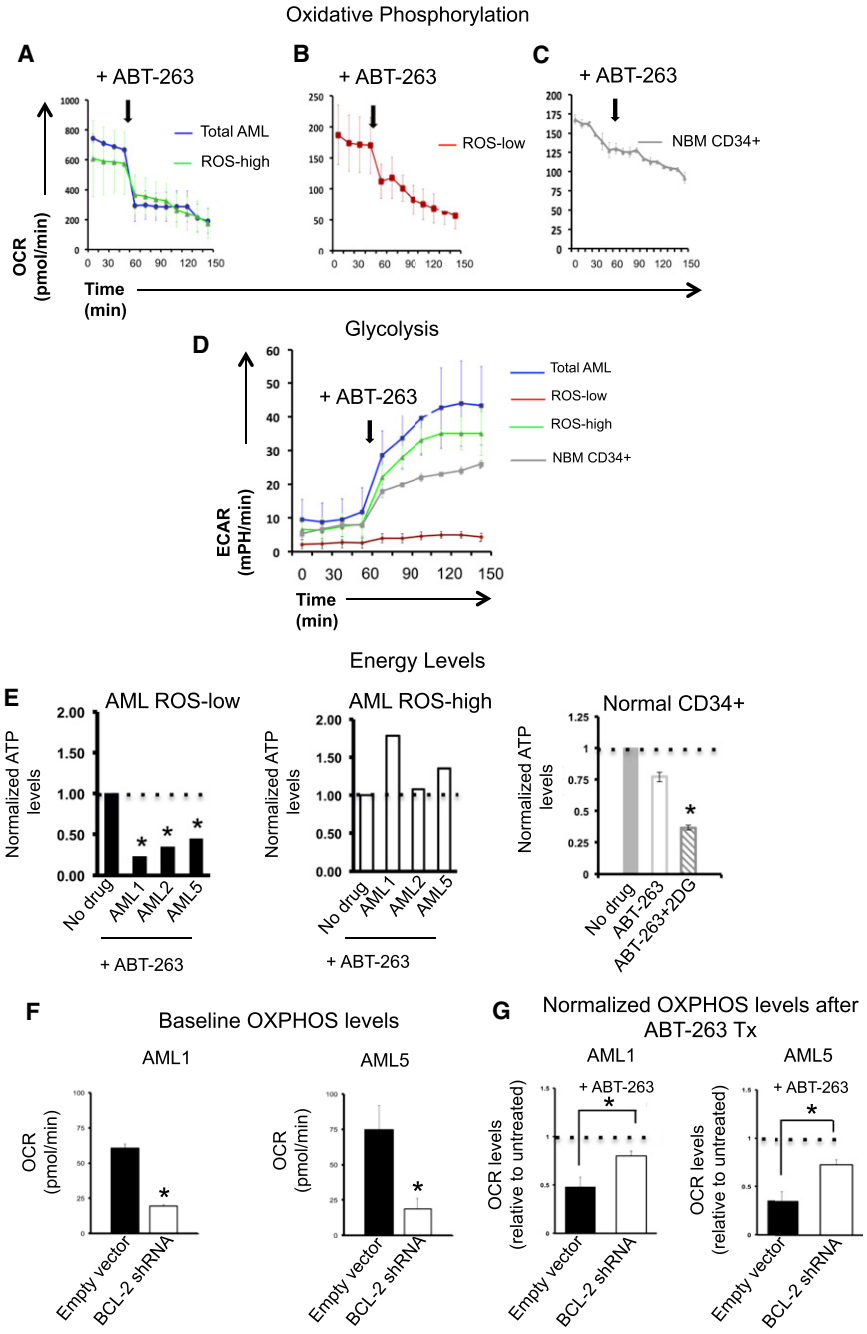

Figure 4. BCL-2 Inhibitors Target LSC Mitochondrial Energy Generation

(A and B) Plots of oxygen consumption rate (OCR, oxidative metabolism) as a parameter of time in the absence (measurements 1–4) and presence (measurements 4–12) of 250nM ABT-263 (indicated by black arrow) in total AML and ROS-high primary AML subsets (A) and in LSC-enriched ROS-low cells (B). Five replicate wells of 1×10^6 total AML, ROS-low, and ROS-high leukemic cells were analyzed. Consecutive measurements (1–12) in both plots were performed every 15 min.

(C) $CD34^+$ cells isolated from normal bone marrow were analyzed similarly to those in (A). See also Figures S4A and S4B.

(D) Extracellular acidification rate (ECAR, glycolytic rate) is plotted as a parameter of time in total AML, ROS-low, and ROS-high subsets, and in normal marrow $CD34^+$ cells in the absence (measurements 1–4) and presence (measurements >4) of 250nM ABT-263.

(E) ATP levels in ROS-low versus ROS-high AML subsets with or without ABT-263 (250nM, 6 hr), and in normal marrow $CD34^+$ cells treated either with ABT-263 alone (250nM, 6 hr) or ABT-263 (250nM) and 2-deoxyglucose (2-DG, 5mM) for 6 hr. Normalized mean values of treated cells as compared to untreated controls (presented as equal to 1) are plotted. *$p \leq 0.05$.

(F) Two independent primary AML specimens were transduced with shRNA targeting BCL-2 by means of lentiviral vectors, as described in the Experimental Procedures. BCL-2 knockdown was confirmed by quantitative RT-PCR (Figure S4C). Baseline OCR indicative of oxidative respiration was analyzed in cells transduced with BCL-2 shRNA and empty vector, and is plotted. Mean ± SEM of two independent experiments are shown. *$p \leq 0.05$.

(G) Primary AML cells transduced with BCL-2 shRNA versus empty vector were treated with ABT-263 (1 μM). OCR values 60 min after treatment are plotted as normalized percentage values of baseline (no drug) values for each sample. Mean ± SEM of two independent experiments are shown. *$p \leq 0.05$. See also Figures S4D–S4F.

Kinetic studies determined that mitochondrial oxidation and glutathione depletion are detectable after 4–6 hr of in vitro exposure of ROS-low cells to BCL-2 pharmacologic inhibitors, and these events occur subsequent to the effects of BCL-2 inhibitors on OXPHOS and the cellular ATP content (not shown). Taken together, our redox and bioenergetic studies showed that BCL-2 inhibition severely impaired LSC redox and energy control. To investigate BCL-2 inhibition as a means for eradicating primitive AML cells, we evaluated the in vitro sensitivity of ROS-low AML to BCL-2 inhibitors. We first used ABT-737, which is a closely related analog of ABT-263 with similar structural features, but which, in contrast to ABT-263, is not orally bioavailable. Those studies showed a dramatic targeting of ROS-low cells with much less effect in the ROS-high compartment (Figure 5B). Additional studies with ABT-263 show consistently strong toxicity to the LSC-enriched ROS-low population with generally less activity toward ROS-high cells, indicating a selective role of BCL-2 in LSC survival (Figure 5D).

To evaluate the relative contribution of ABT-263-induced oxidation in LSC cell death, we investigated whether ROS-low cells would be rescued from BCL-2 inhibitor toxicity by the antioxidants NAC and GSH-ester. NAC and the GSH-ester did not significantly reduce ABT-263 toxicity in ROS-low cells (Figure 5E), indicating the effects of ABT-263 on LSC oxidative state as a late component of the LSC cell death process rather

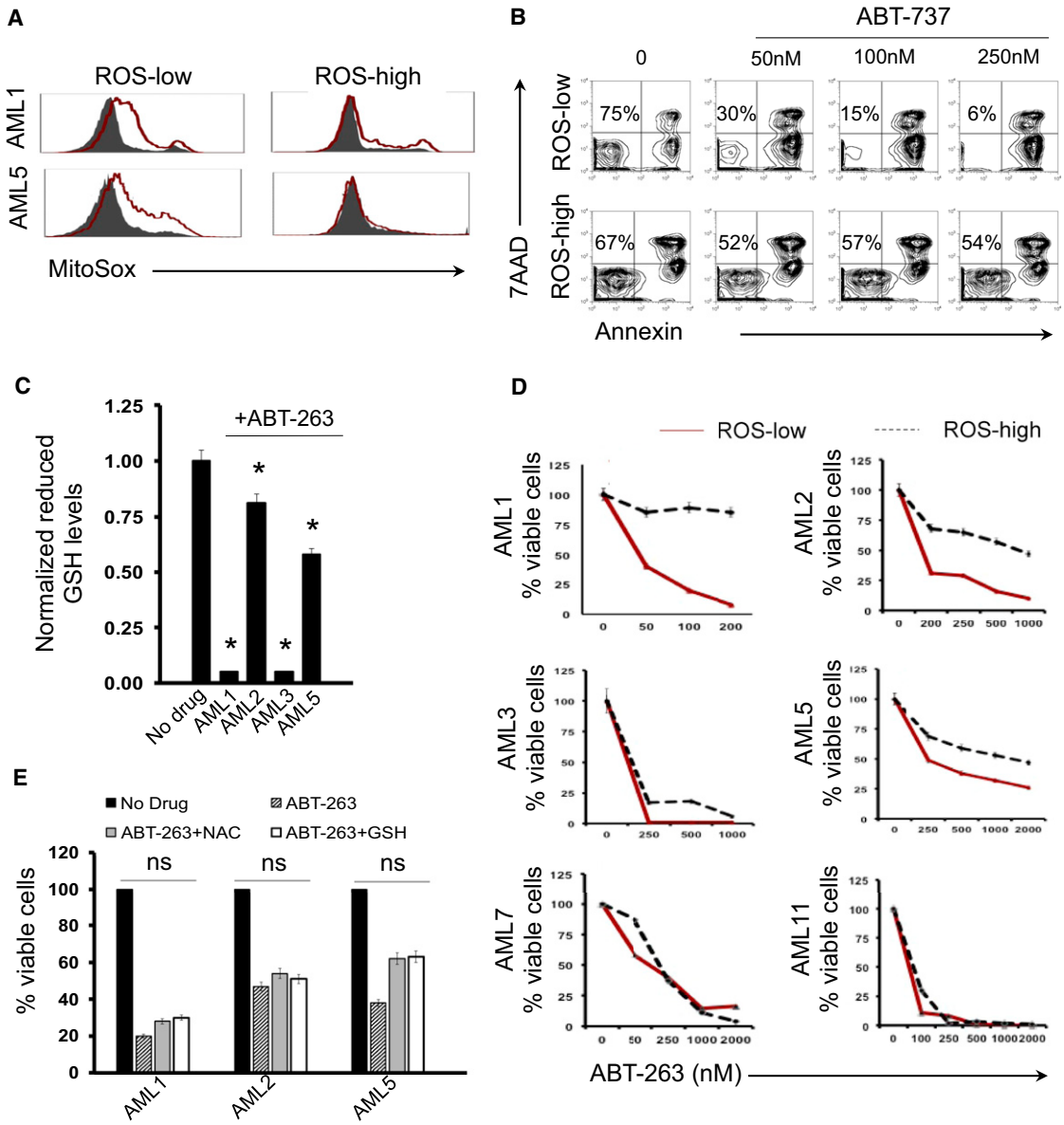

Figure 5. BCL-2 Inhibitors Induce Mitochondrial Oxidation and Cell Death in the LSC Compartment

(A) Mitochondrial ROS, as evaluated by the mitochondrial-specific redox probe MitoSox in ROS-low versus ROS-high AML subsets treated with 250nM ABT-263 for 6 hr. Gray filled, untreated; red line, +ABT-263. See also Figure S5.

(B) Flow cytometric cell death analysis of ROS-low and ROS-high leukemia cells in an AML specimen treated for 18 hr with increasing concentrations of the BCL-2 inhibitor ABT-737. Treated and control cells were labeled with Annexin V and 7AAD and analyzed by flow cytometry. The number of viable ($Ann^-/7AAD^-$) cells is shown.

(C) Reduced GSH levels in primary ROS-low cells subjected to 250nM ABT-263 for 6 hr. Normalized mean values of treated cells as compared to untreated controls (presented as equal to 1) are plotted in n = 4 AML specimens. *$p \leq 0.05$.

(D) In vitro cell death analyses of ROS-low versus ROS-high AML populations in n = 6 AML specimens are shown. Results are expressed as the ratio of the mean viable ($Ann^-/7AAD^-$) treated cells to the mean viable cells of untreated controls. Red, ROS-low; black, ROS-high.

(E) In vitro viability of ROS-low cells treated for 18 hr with 250nM ABT-263 alone, or ABT-263 in combination with 1mM NAC or 1mM GSH-ester. Mean values from duplicate experiments in three independent AML specimens are plotted. *$p \leq 0.05$.

than initiators of cell death. The AML ROS-low cell oxidation following OXPHOS inhibition and cell death induction in response to ABT-263 is not comparable to our findings in steady state conditions, where lower overall and mitochondrial ROS associated with a relatively lower OCR rate (Figure 2A and Figure S2). Further, although ROS-low cells treated with ABT-263 became oxidized, they remained in a quiescent state (Table S4), excluding the possibility of an increase in LSC cell cycle activity as a mechanism of cell death in response to BCL-2 inhibition. Taken together, our findings suggest that BCL-2 inhibitors target LSCs by selectively impairing LSC energy homeostasis.

BCL-2 Inhibition Therapeutically Targets Functionally Defined LSCs

To further investigate BCL-2 inhibition as an approach to target primitive AML cells, we first examined the colony forming potential of primary AML cells transduced with BCL-2 shRNA versus that of control cells. As shown in Figure 6A, BCL-2 knockdown dramatically reduced the colony forming capacity of primary leukemic blasts. Next, we performed xenograft analyses. We treated LSC-enriched ROS-low AML populations in vitro with concentrations of the BCL-2 inhibitor ABT-263 equal to the IC_{50} concentration of the total AML cells for each sample, and then transplanted treated or vehicle control cells into NSG mice. As shown in Figure 6B, ABT-263 reduced LSC potential in all AML specimens evaluated by this functional assay. Importantly, parallel studies performed with the standard chemotherapy agent daunorubicin (DNR), showed almost no activity toward ROS-low LSC engraftment (Figure S6). Next, we also tested the antileukemic effect of pharmacologic BCL-2 inhibitors in vivo by treating mice engrafted with primary human AML cells with ABT-737 (50 mg/kg IP for 15 days). As shown in Figure 6C, ABT-737 clearly reduced leukemia burden in the treated mice. Human leukemic cells isolated from mice that received treatment with ABT-737 were transplanted into secondary recipient mice and demonstrated reduced engraftment compared to leukemic cells from control mice (mean ± SEM: 43.2 ± 5.7 versus 89.2 ± 2.5, $p < 0.05$) (Figure 6D). These findings indicate that in addition to reducing the bulk tumor, ABT-737 targets the LSC compartment. As previously shown (Konopleva et al., 2006), we also found that ABT-263 did not impact the in vitro survival of normal bone marrow $CD34^+$ cells, or the clonogenic potential of normal marrow progenitors (Figures 6E and 6F). Further, functional analysis of total bone marrow mononuclear cells treated overnight in vitro with 250nM ABT-263 and then transplanted in NSG mice showed no significant effect of ABT-263 on the engraftment potential of normal HSCs (Figure 6G). Taken together, these results indicate that BCL-2 inhibition may be an effective means of targeting quiescent ROS-low LSCs.

DISCUSSION

Developing effective strategies to target human LSCs has proven to be a challenging task. While a number of strategies have been proposed based on studies in preclinical models, the clinical utility of such methods remains unclear. An added difficulty that has come to light in recent years is the likely complexity and heterogeneity of the LSC population (Sarry et al., 2011). Evidence from human leukemia studies, as well as related efforts in other cancers, have suggested that the properties defining "stemness" may vary among individual AML patients, as well as within the same patients during the course of disease pathogenesis (Eppert et al., 2011; Sarry et al., 2011). Consequently, it has become increasingly important to determine whether any biological properties are relatively consistent in LSC populations, irrespective of disease stage or the nuances of any individual tumor population. Indeed, fundamental LSC-specific characteristics remain a highly desirable focal point for the development of improved therapies.

In the present study, we examined the properties of LSCs with respect to oxidative status and energy production. In agreement with previous reports on normal stem cells and breast CSCs (Diehn et al., 2009; Jang and Sharkis, 2007; Smith et al., 2000), we observe substantial heterogeneity in LSC oxidative state, an underlying measure of energy metabolism. However, we show that similar to normal stem cell populations (Jang and Sharkis, 2007; Smith et al., 2000), functionally defined LSCs preferentially reside in a reduced state (ROS-low). Our findings in LSC-enriched populations, and previous studies in breast CSCs, indicate a low oxidative state as a potentially frequent CSC property (Diehn et al., 2009). Further, we show here that LSC-enriched populations are characterized by quiescent cell cycle status and low energy production. This relatively dormant condition likely enables LSCs to persist, even under restrictive conditions such as low nutrient or oxygen levels. Intriguingly though, in contrast to our findings in normal $CD34^+$ and previous findings in murine HSCs, both showing that normal stem cells efficiently utilize glycolysis for energy homeostasis (Simsek et al., 2010), ROS-low LSCs appear to be deficient in their ability to employ glycolysis, and are highly reliant on OXPHOS. Glioma stem cells were also shown to be more reliant on oxidative respiration for energy generation, suggesting that lack of glycolytic activity in stem cells may be a broader characteristic of cancers (Vlashi et al., 2011). If true, then therapeutic strategies based on the assumption that tumors are preferentially reliant on glycolysis may need to be reconsidered.

Why ROS-low self-renewing LSC populations, in contrast to the bulk tumor and normal HSCs (Simsek et al., 2010), are less efficient in employing glycolysis represents an important avenue of future investigation. We consider it unlikely that the LSC metabolic profile identified in our study is an artifact of ex vivo cell manipulation, since if this were the case we would expect all leukemic cells to exhibit this phenotype, instead of just the ROS-low subset. Intriguingly, it has been recently proposed that cancer cell subsets with different dependencies in energy-generating pathways coexist within tumors in a symbiotic manner (Nakajima and Van Houten, 2012). In particular, cancer populations that depend on glycolysis for energy generation secrete lactate as a byproduct that is subsequently imported and used as a fuel for oxidative respiration by cancer subsets dependent on oxygen metabolism. Evaluating if this symbiotic model has relevance to the CSC model represents an intriguing line of future investigation. Further, it is possible that the paradoxical OXPHOS dependence of the ROS-low LSC-enriched subset is part of a wider metabolic adaptation of these cells, as they successfully maintain survival despite a dramatically reduced overall metabolic rate. Since oxidative respiration is a slower but significantly more efficient mechanism of energy generation, quiescent LSC subsets may benefit in the long term by using OXPHOS in the context of the tumor microenvironment, as they can more efficiently utilize the limited available nutrients.

By performing gene expression analyses and molecular studies, we show that BCL-2 is preferentially elevated in LSC-enriched ROS-low cells. Although BCL-2 is commonly upregulated in cancer, a differential role for BCL-2 in cancer stem cells has not been widely considered. Notably though, one study by Konopleva et al. (2006) previously demonstrated the activity of BCL-2 inhibitor ABT-737 toward leukemia cells types, including primary AML $CD34^+/CD38^-$ cells. These initial studies first established

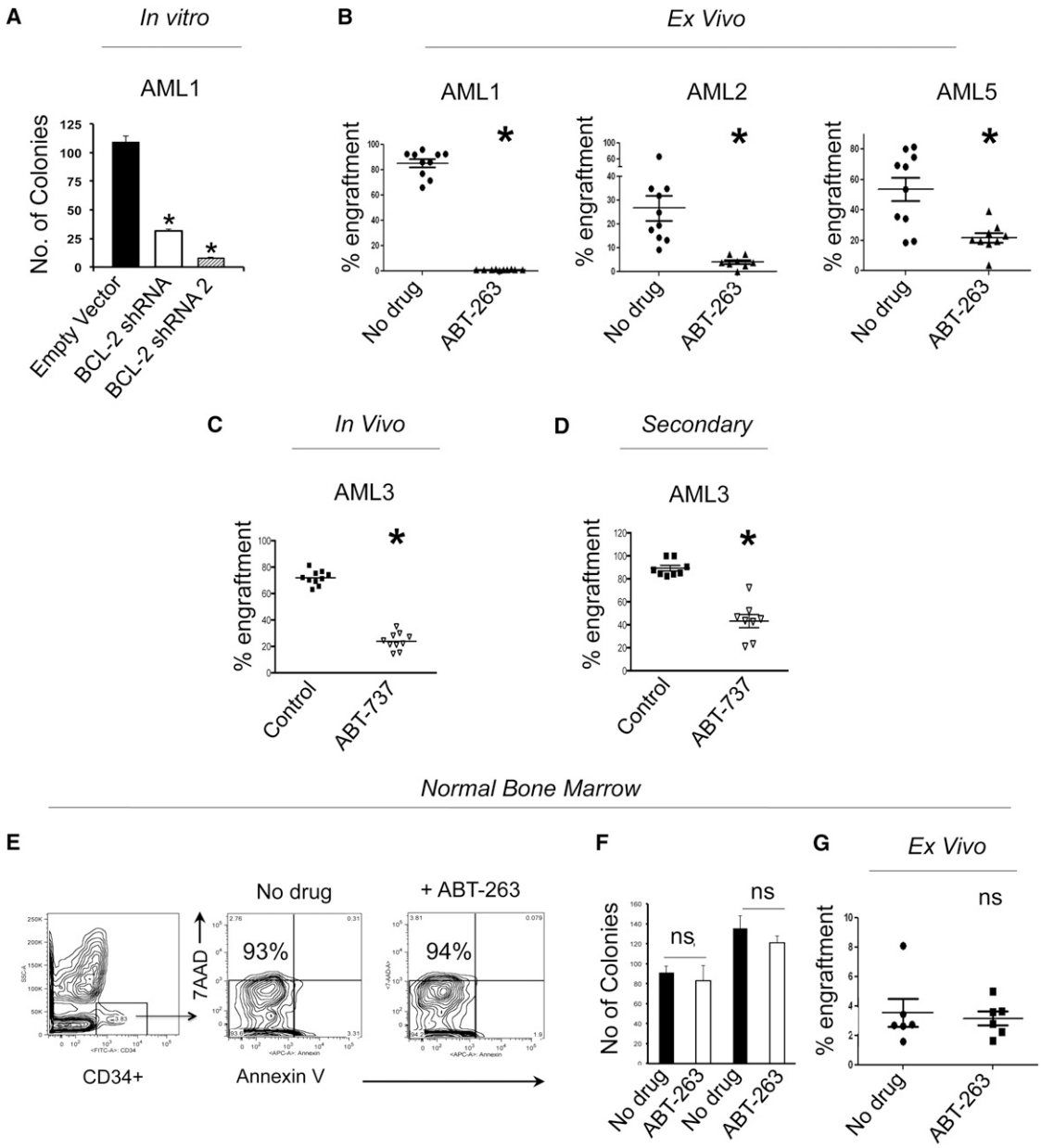

Figure 6. BCL-2 Inhibition Targets Drug-Resistant LSCs

(A) Colony-forming potential of primary AML cells transduced with BCL-2 shRNAs or empty vector. Mean ± SEM values of two independent experiments in triplicate are shown.

(B) Ex vivo cell death analysis of LSC-enriched ROS-low cells treated with ABT-263 in three independent AML specimens. Cells were cultured overnight in vitro with ABT-263 concentrations equal to the IC_{50} drug dose for total AML cells, and then injected into NSG mice. The percentage engraftment of human cells is plotted. *$p \leq 0.05$; ns, not significant. See also Figure S6.

(C) Percentage engraftment of human leukemia cells in NSG mice treated in vivo with vehicle (control) or ABT-737 (50 mg/kg, IP for 14 daily doses).

(D) Human engrafted cells from mice treated in vivo with ABT-737 and respective cells from mice treated with vehicle (control) from the experiment shown in (C) were isolated, and equal numbers of cells were transplanted in secondary recipients. Mice were analyzed for engraftment of human leukemic cells 8 weeks after.

(E) In vitro cell death analysis of normal bone marrow cells treated with ABT-263 (250nM, 18 hr), after gating in the $CD34^+$ hematopoietic progenitor compartment.

(F) Normal bone marrow cells were treated in vitro with ABT-263 (250nM, 18 hr) followed by methylcellulose culture to measure colony formation ability. Mean ± SEM values of two independent experiments in triplicate are shown. ns, not significant.

(G) Ex vivo cell death analysis of normal bone marrow total mononuclear cells cultured overnight in vitro with 250nM ABT-263 and subsequently injected into NSG mice. The percentage engraftment of human cells is plotted.

the concept of using BCL-2 inhibition as a strategy for targeting primitive leukemia cells. Our studies extend the work by Konopleva et al. and provide novel insights on the role of BCL-2 in promoting LSC metabolic homeostasis. Further, by employing xenograft analyses we demonstrate here that both ABT-737 and its optimized orally bioavailable analog, ABT-263, not only decrease bulk leukemia burden, but also target functionally defined LSCs.

From a mechanistic standpoint the high levels of BCL-2 expression we observe in ROS-low cells may promote LSC survival in response to stressful stimuli such as chemotherapy and irradiation by inhibiting the mitochondrial proapoptotic pathway (Del Poeta et al., 2003). In addition, we demonstrate that BCL-2 mediates oxidative respiration, which our findings indicate as essential for LSC energy homeostasis (Figure 7). The role of BCL-2 in promoting mitochondrial bioenergetics offers a unique opportunity for drug targeting in the LSC-specific context, as LSCs not only express high levels of BCL-2 but also have a selective dependency on oxidative respiration. In this vein, we demonstrate that the BCL-2 inhibitors ABT-737 and ABT-263 inhibit LSC oxidative respiration, which is accompanied by selective eradication of ROS-low cells. Importantly, we and others have shown that this class of drugs does not affect normal HSCs (Konopleva et al., 2006). The identification of BCL-2 inhibitors as LSC targeting agents, together with the absence of significant toxicity to normal cells, is intriguing, since it provides a basis for clinical investigation of those drugs at disease stages where targeting residual LSCs is essential, as for instance in consolidation therapy or maintenance treatment during remission.

In conclusion, the concept of targeting cancer cell metabolism has emerged as an intriguing approach to the development of improved therapeutic regimens. We demonstrate here that it is feasible to eradicate resistant LSC populations by targeting their unique metabolic dependencies. Understanding further the metabolic regulation of leukemia stem cells may yield improved therapeutic strategies to eradicate this highly drug-resistant tumor population.

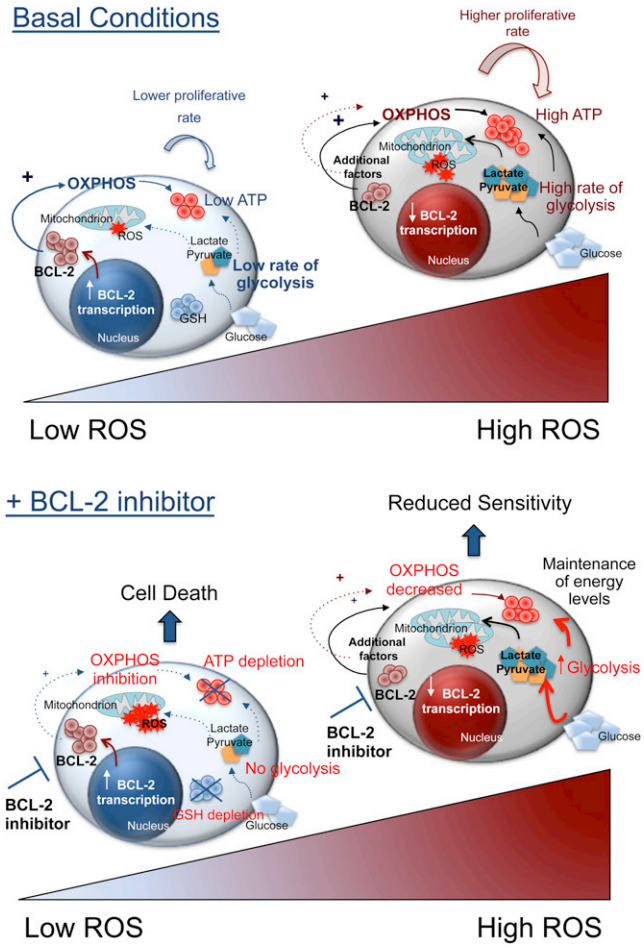

Figure 7. Model for Selective Targeting of LSCs by BCL-2 Inhibition

Upper panel: AML ROS-low cells under baseline conditions are characterized, as compared to AML ROS-high cells, by quiescence, low overall intracellular ROS, low metabolism that generates energy through oxidative respiration rather than glycolysis, and transcriptional upregulation of BCL-2. BCL-2 positively regulates energy generation in AML ROS-low and ROS-high subsets through upregulating oxidative respiration. AML ROS-high cells employ additional mechanisms to maintain a significantly higher metabolic/energetic state as compared to AML ROS-low.

Lower panel: Based on the increased expression of BCL-2 in AML ROS-low cells, and their selective dependency on oxidative respiration for energy homeostasis, upon BCL-2 pharmacologic inhibition by treatment with ABT-263, the OXPHOS of AML ROS-low cells is dramatically reduced, those cells cannot increase glycolysis so as to maintain energy supply, and ATP levels are depleted. This is followed by an increase in mitochondrial ROS, a reduction in cellular glutathione, and the induction of apoptotic cell death. AML ROS-high cells can more efficiently preserve energy supplies in response to BCL-2 pharmacologic inhibition, mainly by upregulating the glycolytic machinery.

EXPERIMENTAL PROCEDURES

Primary AML and Normal Hematopoietic Cells

Normal and leukemic human bone marrow samples were obtained after informed consent from volunteer donors at the University of Rochester Medical Center. Patient clinical characteristics are detailed in Table S1 Total bone marrow mononuclear cells were isolated by standard Ficoll procedures (GE Healthcare, Piscataway, NJ) and cryopreserved in freezing medium consisting of Cryostor CS10 (BioLife Solutions). The viability of leukemic cells after thawing was 50%–90%. Normal bone marrow total mononuclear cells were further enriched for $CD34^+$ cells using MACS CD34 enrichment kit (Milltenyi Biotec, Auburn, CA).

Measurement of Endogenous ROS and Cell Separation Based on ROS Levels

Endogenous ROS levels of primary AML specimens were detected by labeling 1×10^6 leukemic cells for 15 min at 37°C with the redox-sensitive probes CM-H2DCFDA (5μM), CellRox (5μM), MitoSox (5μM), Dihydroethidium (2μM), or Mitotracker (1μM)(Life Technologies). Labeled cells were resuspended in 0.2 ml of 10uM DAPI (Invitrogen) solution and analyzed using BD LSRII flow cytometer (BD Biosciences) and FlowJo software (Treestar).

For cell separation based on endogenous ROS levels, 1×10^8 cells were stained with 10μM CM-H2DCFDA or 8μM CellRox for 15 min at 37°C, washed with PBS with 0.5% FBS, and resuspended in 10uM DAPI solution. Viable AML cells containing lower ROS (bottom 15% of dye distribution) or higher ROS (top 15% of dye distribution) were collected after gating in the $DAPI^-$ population by a BD ARIAII cell sorter (San Jose, CA).

Animal Studies

Sublethally irradiated NSG (NOD.Cg-Prkdcscid Il2rgtm1Wjl/SzJ) mice (Jackson Laboratories, Bar Harbor, ME) were injected with human leukemic cells via tail vein in a final volume of 0.2 ml of PBS with 0.5% FBS. Total AML: sorted

ROS-low: sorted ROS-high cells were transplanted at a constant cell ratio of 5:1:1. Based on the isolation of ROS-low (and respective ROS-high) AML subset as ~15% of the bulk AML cells, this adjustment of the injected cell ratio enables transplantation of approximately equal absolute numbers of ROS-low cells in mice injected with total leukemia cells and in mice injected with purified ROS-low, so as to provide a relative estimate of the contribution of the AML ROS-low cells to the engraftment of the total AML cells.

For secondary transplantation studies of AML specimens, engrafted human cells from mice injected with total, ROS-low, and ROS-high AML cells were adjusted to equal numbers and injected to irradiated NSG secondary recipients. In primary and secondary transplantation experiments, animals were killed after 6–8 weeks and bone marrow was analyzed, by flow cytometry, for the presence of human CD45 and human CD33 to indicate human cells.

Metabolic Assays

O_2 consumption and lactate generation were measured using the Seahorse XF24 extracellular flux analyzer as previously described (Varum et al., 2011). Briefly, five replicate wells of 5×10^5 leukemic or normal cells per well were seeded overnight in 24-well XF24 well plates coated with BD Cell-Tak (BD Biosciences) in serum-free culture medium. One hour prior to analysis, the medium was replaced by unbuffered DMEM and the well plates were incubated to 37°C for pH stabilization. Analyses were performed both at basal conditions and after injection of OLI (1 μg/ml), FCCP (1 μM), Antimycin A (5 μM), ABT-263 (250nM-1 μM), and obatoclax (10 μM). ATP levels were determined according to manufacturer instructions by the ATP Bioluminescence Assay Kit HS II (Roche). The protein expression of the NOX2 (gp91phox) subunit of the NADPH oxidase was detected by flow cytometry after cells were labeled with anti-NOX2 antibody (bs-3889R, Bios USA) as previously described (Hole et al., 2010).

In Vivo Treatment of Xenografts with ABT-737

Irradiated NSG mice were transplanted with human leukemia cells (3×10^6/mouse) via tail vein in a final volume of 0.2 ml of PBS with 0.5% FBS. After 2 weeks, animals were size-matched to treatment and control groups (10 animals per group) and received either ABT-737 (50 mg/kg, IP for 14 daily doses) or vehicle. ABT-737 was formulated in 30% propylene glycol, 5% Tween 80, and 65% dextrose and prepared freshly every day. After treatment, mice were sacrificed and human engrafted cells were evaluated by flow cytometry.

SUPPLEMENTAL INFORMATION

Supplemental Information for this article includes six figures, four tables, and Supplemental Experimental Procedures and can be found with this article online at http://dx.doi.org/10.1016/j.stem.2012.12.013.

ACKNOWLEDGMENTS

The authors gratefully acknowledge critical review and comments by Drs. Fay Young, H. Leighton Grimes, Martin Carroll, and Helene McMurray, and technical assistance by the Functional Genomics Center of the University of Rochester. Craig Jordan is supported by an endowed chair generously provided by Philip and Marilyn Wehrheim. Research studies described in this manuscript were supported by grants from the Leukemia and Lymphoma Society (6230-11 and 6133-12, C.T.J.), NYSTEM (CO24964, C.T.J.), and the US National Institutes of Health (HL-071158, P.S.B.).

Received: July 17, 2012
Revised: November 5, 2012
Accepted: December 17, 2012
Published: January 17, 2013

REFERENCES

Cairns, R.A., Harris, I.S., and Mak, T.W. (2011). Regulation of cancer cell metabolism. Nat. Rev. Cancer *11*, 85–95.

Chen, Z.X., and Pervaiz, S. (2007). Bcl-2 induces pro-oxidant state by engaging mitochondrial respiration in tumor cells. Cell Death Differ. *14*, 1617–1627.

Del Poeta, G., Venditti, A., Del Principe, M.I., Maurillo, L., Buccisano, F., Tamburini, A., Cox, M.C., Franchi, A., Bruno, A., Mazzone, C., et al. (2003). Amount of spontaneous apoptosis detected by Bax/Bcl-2 ratio predicts outcome in acute myeloid leukemia (AML). Blood *101*, 2125–2131.

Delia, D., Aiello, A., Soligo, D., Fontanella, E., Melani, C., Pezzella, F., Pierotti, M.A., and Della Porta, G. (1992). bcl-2 proto-oncogene expression in normal and neoplastic human myeloid cells. Blood *79*, 1291–1298.

Diehn, M., Cho, R.W., Lobo, N.A., Kalisky, T., Dorie, M.J., Kulp, A.N., Qian, D., Lam, J.S., Ailles, L.E., Wong, M., et al. (2009). Association of reactive oxygen species levels and radioresistance in cancer stem cells. Nature *458*, 780–783.

Eppert, K., Takenaka, K., Lechman, E.R., Waldron, L., Nilsson, B., van Galen, P., Metzeler, K.H., Poeppl, A., Ling, V., Beyene, J., et al. (2011). Stem cell gene expression programs influence clinical outcome in human leukemia. Nat. Med. *17*, 1086–1093.

Falini, B., Nicoletti, I., Martelli, M.F., and Mecucci, C. (2007). Acute myeloid leukemia carrying cytoplasmic/mutated nucleophosmin (NPMc+ AML): biologic and clinical features. Blood *109*, 874–885.

Hole, P.S., Pearn, L., Tonks, A.J., James, P.E., Burnett, A.K., Darley, R.L., and Tonks, A. (2010). Ras-induced reactive oxygen species promote growth factor-independent proliferation in human CD34+ hematopoietic progenitor cells. Blood *115*, 1238–1246.

Ito, K., Hirao, A., Arai, F., Takubo, K., Matsuoka, S., Miyamoto, K., Ohmura, M., Naka, K., Hosokawa, K., Ikeda, Y., and Suda, T. (2006). Reactive oxygen species act through p38 MAPK to limit the lifespan of hematopoietic stem cells. Nat. Med. *12*, 446–451.

Jang, Y.Y., and Sharkis, S.J. (2007). A low level of reactive oxygen species selects for primitive hematopoietic stem cells that may reside in the low-oxygenic niche. Blood *110*, 3056–3063.

Konopleva, M., Contractor, R., Tsao, T., Samudio, I., Ruvolo, P.P., Kitada, S., Deng, X., Zhai, D., Shi, Y.X., Sneed, T., et al. (2006). Mechanisms of apoptosis sensitivity and resistance to the BH3 mimetic ABT-737 in acute myeloid leukemia. Cancer Cell *10*, 375–388.

Magee, J.A., Piskounova, E., and Morrison, S.J. (2012). Cancer stem cells: impact, heterogeneity, and uncertainty. Cancer Cell *21*, 283–296.

Nakajima, E.C., and Van Houten, B. (2012). Metabolic symbiosis in cancer: Refocusing the Warburg lens. Mol. Carcinog. Published online January 6, 2012. http://dx.doi.org/10.1002/mc.21863.

Saito, Y., Uchida, N., Tanaka, S., Suzuki, N., Tomizawa-Murasawa, M., Sone, A., Najima, Y., Takagi, S., Aoki, Y., Wake, A., et al. (2010). Induction of cell cycle entry eliminates human leukemia stem cells in a mouse model of AML. Nat. Biotechnol. *28*, 275–280.

Sarry, J.E., Murphy, K., Perry, R., Sanchez, P.V., Secreto, A., Keefer, C., Swider, C.R., Strzelecki, A.C., Cavelier, C., Récher, C., et al. (2011). Human acute myelogenous leukemia stem cells are rare and heterogeneous when assayed in NOD/SCID/IL2Rγc-deficient mice. J. Clin. Invest. *121*, 384–395.

Simsek, T., Kocabas, F., Zheng, J., Deberardinis, R.J., Mahmoud, A.I., Olson, E.N., Schneider, J.W., Zhang, C.C., and Sadek, H.A. (2010). The distinct metabolic profile of hematopoietic stem cells reflects their location in a hypoxic niche. Cell Stem Cell *7*, 380–390.

Smith, J., Ladi, E., Mayer-Proschel, M., and Noble, M. (2000). Redox state is a central modulator of the balance between self-renewal and differentiation in a dividing glial precursor cell. Proc. Natl. Acad. Sci. USA *97*, 10032–10037.

Tothova, Z., Kollipara, R., Huntly, B.J., Lee, B.H., Castrillon, D.H., Cullen, D.E., McDowell, E.P., Lazo-Kallanian, S., Williams, I.R., Sears, C., et al. (2007). FoxOs are critical mediators of hematopoietic stem cell resistance to physiologic oxidative stress. Cell *128*, 325–339.

Trachootham, D., Zhang, H., Zhang, W., Feng, L., Du, M., Zhou, Y., Chen, Z., Pelicano, H., Plunkett, W., Wierda, W.G., et al. (2008). Effective elimination of fludarabine-resistant CLL cells by PEITC through a redox-mediated mechanism. Blood *112*, 1912–1922.

Trachootham, D., Alexandre, J., and Huang, P. (2009). Targeting cancer cells by ROS-mediated mechanisms: a radical therapeutic approach? Nat. Rev. Drug Discov. *8*, 579–591.

van Delft, M.F., Wei, A.H., Mason, K.D., Vandenberg, C.J., Chen, L., Czabotar, P.E., Willis, S.N., Scott, C.L., Day, C.L., Cory, S., et al. (2006). The BH3 mimetic ABT-737 targets selective Bcl-2 proteins and efficiently induces apoptosis via Bak/Bax if Mcl-1 is neutralized. Cancer Cell *10*, 389–399.

Varum, S., Rodrigues, A.S., Moura, M.B., Momcilovic, O., Easley, C.A., 4th, Ramalho-Santos, J., Van Houten, B., and Schatten, G. (2011). Energy metabolism in human pluripotent stem cells and their differentiated counterparts. PLoS ONE *6*, e20914.

Vlashi, E., Lagadec, C., Vergnes, L., Matsutani, T., Masui, K., Poulou, M., Popescu, R., Della Donna, L., Evers, P., Dekmezian, C., et al. (2011). Metabolic state of glioma stem cells and nontumorigenic cells. Proc. Natl. Acad. Sci. USA *108*, 16062–16067.

Warburg, O. (1956). On the origin of cancer cells. Science *123*, 309–314.

Westermann, B. (2010). Mitochondrial fusion and fission in cell life and death. Nat. Rev. Mol. Cell Biol. *11*, 872–884.